DETERMINATION OF FLUID FORCES ON A CIRCULAR CYLINDER IN PULSATING CROSS-FLOW FROM NUMERICAL EXPERIMENTS

Chunlei Liang
Department of Aeronautics and Astronautics, Stanford University, Stanford, United States
Efstathios Konstantinidis
Department of Engineering and Management of Energy Resources, University of Western Macedonia, Kozani, Greece

ABSTRACT

Three-dimensional large-eddy simulations of pulsating flow about a circular cylinder were performed at a Reynolds number of 2580. The amplitude of the pulsations is set at 5% of the mean flow velocity and the pulsation frequency is varied around twice the frequency of vortex shedding in steady flow. The results show that a mean drag peak amplification occurs at a critical excitation frequency which compares well to available experimental data. The fluctuating drag and lift coefficients are reported and their phase relationship with respect to the imposed pulsation and the vortex dynamics in the wake is discussed.

1. INTRODUCTION

Forces on bluff cylinders in cross-flow have been studied extensively due to their importance in engineering applications and associated flow-induced vibration problems such as, for example, in shell-and-tube heat exchangers, offshore risers, etc. In practical situations, the incident flow may have a pulsating component superimposed on the average flow velocity, e.g., in flows delivered by reciprocating pumps or in systems where surging may occur for internal flows, or by combination of currents and waves in offshore applications. Aside from its practical importance, pulsed flow over a circular cylinder offers a generic configuration to study and improve understanding of more complex fluid-structure interactions. Previous work has demonstrated the existence of *vortex shedding lock-on* for excitation frequencies around twice the natural wake frequency (Barbi et al, 1986). The effects accompanying lock-on have also received attention (see Konstantinidis et al, 2003, and references cited therein). However, a survey of the published literature indicates a lack of data for the fluctuating forces on a circular cylinder in pulsating cross-flow.

The objective of the present work is to investigate the effects of a small pulsation superimposed onto a steady flow on the vortex shedding, vortex patterns and forces on a stationary cylinder in the subcritical Reynolds number regime. Since the phenomenon of a cylinder oscillating in a steady flow is analogous to that of a cylinder subjected to an oscillating flow, the present investigation also seeks to give some information on the effects of vortex-induced in-line vibration. This approach allows one to concentrate solely on the vortex dynamics in the wake.

2. FORCES IN PULSATING FLOW

Consider a fixed bluff cylinder placed normal to a pulsating flow $U(t) = U_m + U_o \sin(2\pi f_o t)$, where U_m is the mean flow velocity, f_o and U_o are the frequency and amplitude of pulsation, respectively. The inline fluid force per unit length is considered to be the sum of an inertial and a drag force in the so-called Morison equation (Blevins, 2001),

$$F_x = \tfrac{1}{4}\rho\pi D^2 C_m \dot{U} + \tfrac{1}{2}\rho D\,|U|\,U C_d, \qquad (1)$$

where ρ is the fluid density, D is the cylinder diameter, C_m and C_d are the inertia and drag coefficients, respectively. The dot denotes derivative with respect to time. The inertial force accounts for two different mechanisms: (a) a component due to the pressure waves induced by the pulsations, and (b) a component due to the added mass. The coefficients C_m and C_d in Eq. (1) are assumed constant over a cycle but they will be functions of three independent parameters $U_m D/\nu$ ($= Re$, the Reynolds number; ν is the kinematic viscosity of the fluid), $U_o/f_o D$, and $f_o D/U_m$. Depending on the relative magnitude of the coefficients there exist two different regimes: for relatively low amplitudes ($U_o/f_o D < 5$) the total force is dominated by the inertia

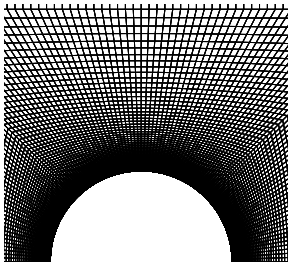

Figure 1: *Close-up view of a slice of the computational mesh near the cylinder surface.*

force while for high amplitudes ($U_o/f_oD > 25$) the drag force dominates. For intermediate amplitudes ($5 < U_o/f_oD < 25$), both the inertia and drag force are important. The present study concerns the lower end of the inertia-dominated regime ($U_o/f_oD \ll 5$) and complements previous work concerned with the intermediate regime which has been dealt with previously by Zhou and Graham (2000).

3. NUMERICAL METHOD

For the present study, large-eddy simulations were carried out on a three-dimensional unstructured collocated grid to predict the velocity and pressure field of pulsating cross-flow around a circular cylinder in primitive variables. The incompressible Navier-Stokes equations were low-pass filtered in space and the standard Smagorinsky eddy viscosity model was used for the unresolved scales ($C_S = 0.1$). A finite-volume method with second-order central-difference scheme was employed for the spatial discretization on an unstructured collocated grid comprising 746,688 cells per plane. A close-up view of the computational mesh near the cylinder surface is shown in Fig. 1. A dense mesh is used in this region in order to resolve the growth of the boundary layer and its separation. The total dimensions of the mesh are $18.8D$ and $10D$ along the flow direction and transverse to it, respectively. The cylinder is πD long and 32 planes were employed along the span. A second-order accurate Crank-Nicholson scheme was employed for time advancement. More details on the numerical scheme and grid independence studies can be found in Liang and Papadakis (2007). Table 1 shows a comparison of the global wake parameters computed from the present numerical scheme to experimental data (Konstantinidis et al, 2005). Extensive comparisons of the velocity wake field have also been made and good agreement was found as reported elsewhere (Liang and Papadakis, 2007, Konstantinidis et al, 2007).

	Re	St	C_{dm}
PIV	2140	0.215	1.19
LES	2580	0.225	1.24

Table 1: *Global wake parameters in steady flow.*

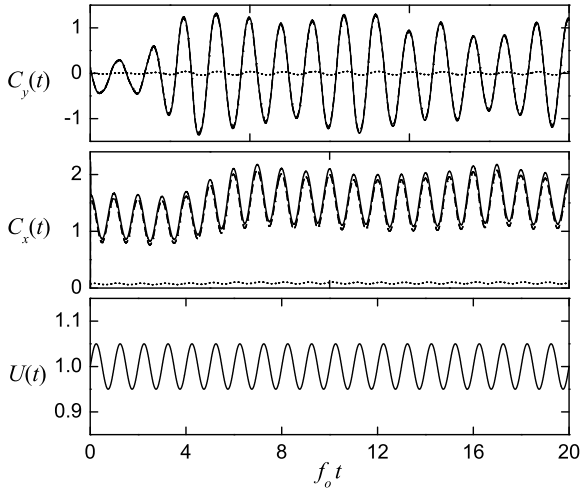

Figure 2: *Result from a typical run; $f_o/f_v = 2.0$.*

4. NUMERICAL RESULTS

A number of computations were performed for pulsation frequencies around twice the natural vortex shedding frequency in steady flow, f_v, for which a strong interaction might be expected due the lock-on phenomenon (Konstantinidis et al. 2003). The objective is to determine the variation of the mean and fluctuating forces on the cylinder with pulsation frequency over relatively small increments. For the present computations, the Reynolds number based on mean inflow velocity is 2580 and the pulsation amplitude is kept constant at $U_o/U_m = 0.05$.

4.1. Time history of forces

Fig. 2 shows the time trace of the forces exerted on the cylinder from a typical run for $f_o/f_v = 2.0$. Computations start at $t = 0$ from the steady flow solution. After an initial transient the total drag $C_x(t)$ and lift $C_y(t)$ coefficients become synchronized with the imposed frequency of pulsation

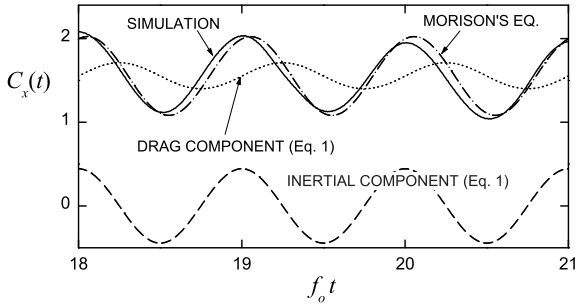

Figure 3: *Comparison between presnt simulations and Morison's equation for* $f_o/f_v = 2.0$.

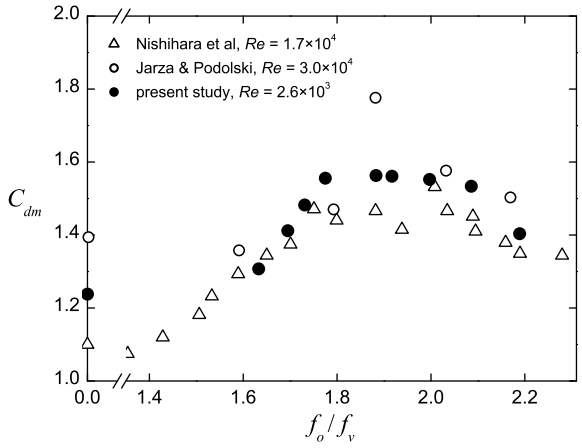

Figure 4: *Variation of the mean drag coefficient with pulsation/natural vortex shedding frequency ratio.*

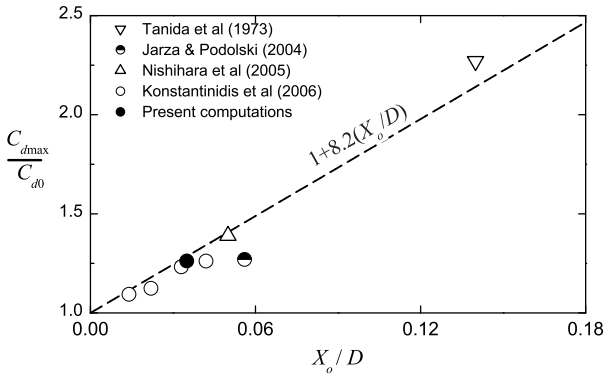

Figure 5: *Mean drag amplification with amplitude of equivalent inline cylinder oscillation.*

and their fluctuation magnitude increases compared to steady flow. The dotted and dashed lines show the contributions of the skin friction and pressure distribution around the cylinder to the total forces. Clearly, the contribution of skin friction is negligible.

In Fig. 3, a comparison is made between the present simulations for $f_o/f_v = 2.0$ and the Morison equation (Eq. 1) for $f_o/f_v = 2.0$. For the purposes of the present analysis, the inertia coefficient is that resulting from potential flow theory ($C_m = 1 + C_a = 2$; C_a is the added mass coefficient) and C_d is equal to the mean drag computed from the numerical results. Eq. 1 predicts the mean and fluctuation of the inline force quite well although the phase is not accurately predicted. At different frequency ratios the prediction of the phase deteriorates due to variations in the actual or effective added mass (Sarpkaya, 2004, Williamson and Govardhan, 2004). Of course, it is common to fit the coefficients to the data in order to achieve better agreement (see, e.g., Zhou and Graham, 2000). As it is shown further below, the apparent success of Morison's equation in the low inertia-dominated regime conceals the physics of the separated wake flow.

4.2. Mean drag force

Fig. 4 shows the variation of the mean drag coefficient *vs.* the pulsation/natural shedding frequency ratio from different runs. It should be clarified that the mean drag is the long time-average of the total inline force per unit length appropriately normalized, i.e.,

$$C_{dm} = \frac{\frac{1}{T}\int_0^T F_x(t)\mathrm{d}t}{\frac{1}{2}\rho D U_m^2} \qquad (2)$$

There is a range of frequency ratios centered at $f_o/f_v \approx 1.9$ for which the mean drag coefficient exhibits a peak amplification (the magnitude of the increase is discussed further below). The centre frequency is termed 'critical' and denoted f_o^*/f_v hereforth for reasons that will become clear further below. Comparison is made to experimental data from inline cylinder oscillations in steady flow (Nishihara et al. 2005) and from a fixed cylinder in pulsating flow (Jarza and Podolski, 2004) for similar perturbation amplitudes ($U_o/U_m \approx 0.05$). The present computations agree well with the experimental data, particularly if the difference in the mean drag for steady flow is taken into account. It should be emphasized that the collapse of the peak would be less satisfactorily if a different abscissa was employed, e.g. $f_o D/U_m$ instead of f_o/f_v which effectively absorbs the sensitivity of the Strouhal number to experimental/computational setup.

In order to compare the peak amplification

data from a stationary cylinder in pulsating flow to the analogous case of a cylinder oscillating inline with a steady flow, we introduce the equivalent normalized amplitude of oscillation, $X_o/D = U_o/2\pi f_o D$ and the normalized mean drag C_{dm}/C_{d0} where C_{d0} is the drag coefficient in steady flow. Fig. 5 shows the present data together with experimental data from inline cylinder oscillations in steady flow (triangles) and from a fixed cylinder in pulsating flow (circles). Although most of the available data are limited to low amplitudes $X_o/D < 0.06$, a linear relationship seems to represent the data trend correctly. This trend indicates that the wake response of a cylinder in pulsating flow is equivalent to that from a cylinder oscillating inline with a steady flow. It is well-known that for transverse cylinder oscillations a similar linear increase with amplitude is observed (see Blevins, 2001, p. 58). However, the rate of mean drag amplification with normalized amplitude is about one-fourth of that reported here.

4.3. Fluctuating forces

Fig. 6 shows the r.m.s. fluctuation of the force coefficients in the inline and transverse directions, C_x and C_y respectively. A dashed line shows the contribution of the inertia term in Eq. (1) to the total inline force, where the inertia coefficient is that resulting from potential flow theory as discussed above. As it would be expected, C_x is dominated by the inertial component. The r.m.s. fluctuation of the inline force coefficient is only slightly overpredicted by Eq. (1) as seen in Fig. 6 and the use of Morison's equation to predict the fluctuating force magnitude (but not the phase) would seem justified even without fitting of the coefficients. However, the r.m.s. fluctuation of C_x does not increase monotonically with f_o/f_v due to variations in the actual added mass. The r.m.s. of the transverse force coefficient also displays a broad peak at f_o^*/f_v, similar to that of the mean drag, with peak values nearly four times higher than the steady flow counterpart. It might be noted that C_y is seemingly free from inertial effects and therefore more representative of the vortex dynamics in the wake.

4.4. Phase of the inline force

As pointed out by Bearman (1984) the magnitude of the fluctuating forces on a stationary bluff-body *"will give little indication of the likely amplitudes of motion of similar bodies flexibly mounted"*. In view of the importance of the phase

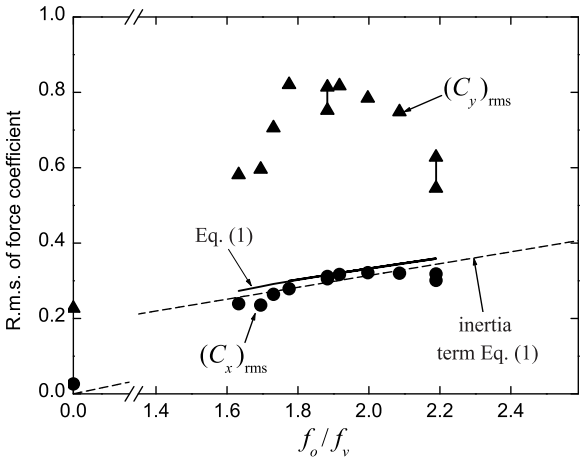

Figure 6: *Variation of the fluctuating forces with pulsation/natural shedding frequency ratio.*

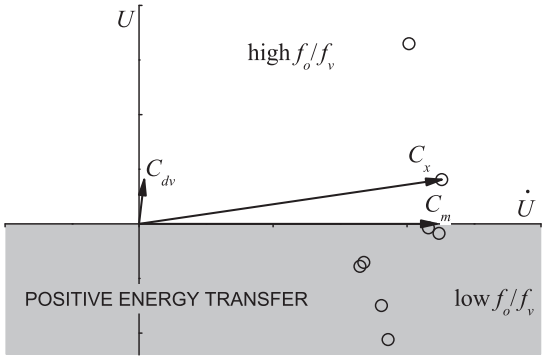

Figure 7: *Phase diagram showing the phase relationship between $C_x(t)$ and $U(t)$. Vectors show the force components for $f_o/f_v = 2.0$.*

of the forces with respect to the velocity of the fluid relative to the body for the energy transfer mechanism, we employed cross-spectral analysis to determine the phase ϕ between $C_x(t)$ and $U(t)$. The results show that $\phi \approx \pi/2$ within the synchronization range. This might be expected due to the dominance of the inertial component on the total force. Frequency ratios lower than the critical ($f_o^*/f_v \approx 1.9$) induce a phase slightly above $\pi/2$ whereas for frequencies higher than the critical the phase is slightly less than $\pi/2$. At f_o^*/f_v, the mean drag and fluctuating lift coefficients become maximum and $\phi = \pi/2$. The computed values of ϕ are shown schematically in the phase diagram of Fig. 7. Note that U and $\dot{U}$ are the velocity and acceleration of the fluid and the phase is positive for clockwise rotation. Also, the vertical axis is exaggerated for clarity.

The present computations suggest that the

magnified forces due to vortex shedding lock-on can only sustain self-excited inline vibrations of compliant structures, e.g. elastically supported cylinders, only for frequency ratios lower than the critical one. At frequency ratios higher than the critical one, the phase of the drag force induces a negative excitation (positive damping), i.e. energy is transferred from the structure to the fluid as shown graphically in Fig. 7. This further substantiates the arguments by Konstantinidis et al (2005) that the gradual change in the timing of vortex shedding across the synchronization range, which effectively determines the phase of the fluctuating forces, suppresses the inline vortex-induced vibrations of elastically-supported cylinders near the middle of the synchronization as observed in related studies.

It is intriguing to decompose the total inline force to an apparent mass force (the potential added mass) and a 'vortex drag' force as in the case of transverse cylinder oscillations (Williamson and Govardhan, 2004). The vector diagram in Fig. 7 shows the vortex drag coefficient C_{dv} resulting from the above decomposition. In the particular example shown, which corresponds to a high frequency ratio, C_{dv} would be almost in-phase with the flow velocity U. However, as discussed in the next section, there is no evident component of the drag force related to the vortex dynamics in the wake with such a phasing.

4.5. Phase-averaged flow field

In order to relate the forces exerted on the cylinder to the vortex dynamics in the wake, Fig. 8 shows a representative sequence of phase-averaged velocity vectors and pressure fields around the body for $f_o/f_v = 2.0$. The lower plot shows the corresponding instants in the pulsation cycle (note that one vortex shedding cycle corresponds to two pulsation cycles during synchronization). It should also be noted that the velocity vectors shown are interpolated onto a coarser mesh for clarity. During the phases shown (a–d), an anti-clockwise vortex is formed on the lower side of the cylinder. As the vortex grows in size during formation, it moves towards the base of the cylinder and produces a region of low pressure near the cylinder surface. The pressure distribution in phase (b) indicates that the base pressure coefficient becomes lower than in the remainder of the pulsation cycle and therefore the drag force is maximized just after the end of each pulsation cycle (in agreement with the phase determined by spectral analysis). At the same phase, the velocity just outside the separation point on the lower side attains its maximum value ($\approx 1.75U_m$) and it can be inferred from Bernoulli's principle that the pressure on the same side attains its lowest value. As a result, the lift force peaks at this phase pointing towards the bottom.

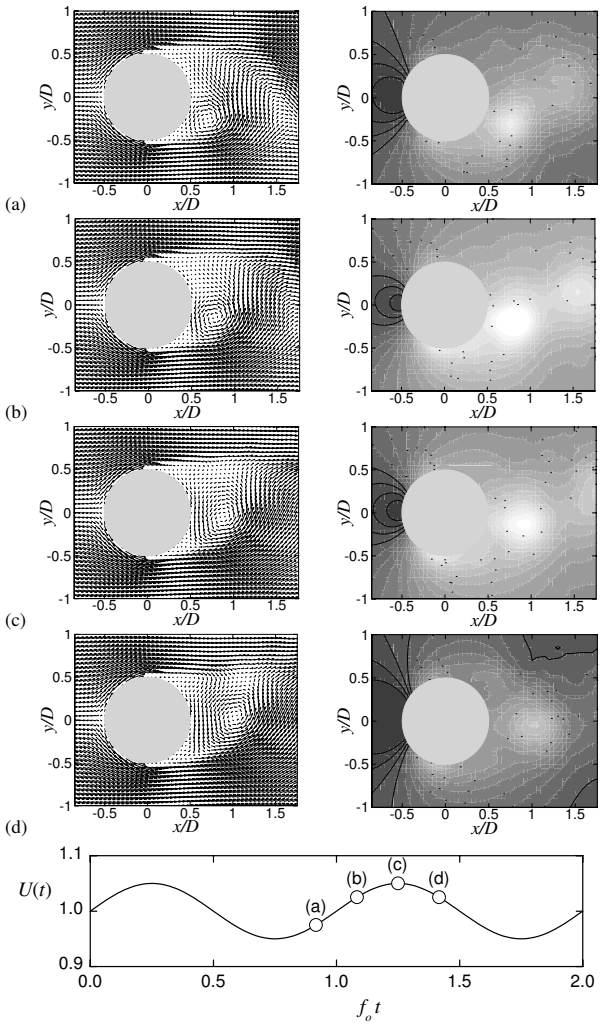

Figure 8: *Phase-averaged velocity vectors and pressure distribution around the cylinder for* $f_o/f_v = 2.0$. *Dark and light shading indicates a positive and negative pressure coefficient respectively.*

The above description illustrates how the vortex formation and shedding process relates to the generation of forces on the cylinder. As noted by Konstantinidis et al (2005), the timing of vortex shedding is shifted earlier in the periodic cycle for low frequency ratios and vice versa at high frequency ratios. As a result, the phase of the forces *vis-à-vis* the relative velocity between the fluid and the structure exhibits a systematic change within the synchronization range. Furthermore,

the present findings provide some evidence that there is a critical frequency ratio f_o^*/f_v within the synchronization range at which the mean and fluctuating forces exhibit a peak amplification and the phase relationship between the vortex-induced forces and the velocity of the fluid *vis-à-vis* the body are universal features of synchronized bluff-body wakes (see Carberry et al, 2005, for related data from a cylinder in transverse oscillation).

5. CONCLUSION

The present large-eddy simulations agree well with available experimental data obtained in similar configurations. The results support the view that the wake response and the vortex dynamics from a cylinder in pulsating flow are equivalent to that of a cylinder oscillating inline with a steady flow. There is a critical frequency of excitation at which the mean drag and the fluctuating lift forces exhibit a peak amplification. Therefore, the mean drag force provides a useful diagnostic tool to assess the state of the wake. The Morison equation taken in tandem with the drag amplification linear fit provide a means to predict the maximum fluctuating loads on cylindrical structures due to flow pulsations (but not the phase of the inline force). Although the magnified fluid forces due to vortex shedding lock-on have the potential to destabilize a structure, they can only sustain the vibration of compliant structures for frequencies less than the critical; for frequencies above the critical, the phase of the inline force *vis-a-vis* the velocity of the fluid which is determined by timing of vortex shedding, induces a negative excitation.

Acknowledgement E.K. would like to thank Dr Takashi Nishihara for the provision of his data and for helpful discussions regarding aspects of the present work.

6. REFERENCES

Barbi, C., et al, 1986, Vortex shedding and lock-on of a circular cylinder in oscillatory flow. *Journal of Fluid Mechanics*, **170**: 527–544.

Bearman, P.W., 1984, Vortex shedding from oscillating bluff bodies. *Annual Review of Fluid Mechanics*, **16**: 195–222.

Blevins, R.D., 2001, *Flow-Induced Vibration*, Reprint edition, Krieger Publishing Co.

Carberry, J., et al, 2005, Controlled oscillations of a cylinder: forces and wake modes. *Journal of Fluid Mechanics*, **538**: 31–69.

Jarza A. and Podolski M., 2004, Turbulence structure in the vortex formation region behind a circular cylinder in lock-on conditions. *European Journal of Mechanics B/Fluids*, **23**: 535–550.

Konstantinidis, E., et al, 2003, The effect of flow perturbations on the near wake characteristics of a circular cylinder. *Journal of Fluids and Structures*, **18**: 367–386.

Konstantinidis, E., et al, 2005, The timing of vortex shedding in a cylinder wake imposed by periodic inflow perturbations. *Journal of Fluid Mechanics*, **543**: 45–55.

Konstantinidis, E., et al, 2006, The effect of forcing amplitude on vortex strength, drag and Reynolds stresses in the wake of a cylinder in oscillating flow. Presented at *Euromech Fluid Mechanics Conference*, June 26–30, Stockholm, Sweden.

Konstantinidis, E., et al, 2007, Control of the separated flow behind a circular cylinder by flow forcing. In *IUTAM Symposium on Unsteady Separated Flows and their Control*, June 18-22, Corfu, Greece.

Liang, C. and Papadakis, G., 2007, Large eddy simulation of pulsating flow over a circular cylinder at subcritical Reynolds number. *Computers and Fluids*, **36**: 299–312.

Nishihara, T., et al, 2005, Characteristics of fluid dynamic forces acting on a circular cylinder oscillated in the streamwise direction and its wake patterns. *Journal of Fluids and Structures*, **20**: 505–518.

Sarpkaya, T., 2004, A critical review of the intrinsic nature nature of vortex-induced vibrations. *Journal of Fluids and Structures*, **19**: 389–447.

Tanida, Y., et al, 1973, Stability of a circular cylinder oscillating in uniform flow or in a wake. *Journal of Fluid Mechanics*, **61**: 769–784.

Williamson, C. H. K. and Govardhan, R., 2004, Vortex-induced vibrations. *Annual Review of Fluid Mechanics*, **36**: 413–455.

Zhou, C.Y. and Graham M.R., 2000, A numerical study of cylinders in waves and currents. *Journal of Fluids and Structures*, **14**: 403–428.